

4. Result and Discussion

Several standard metrics were employed to determine their performance in assessing AD Detection and classification models. Accuracy evaluates how well the model consistently makes accurate predictions. Correctly identified cases (true positives and true negatives) are combined and then divided by the total number of occurrences in the dataset to determine the accuracy rate. However, if the dataset has an uneven distribution of classes, the accuracy metric may not be an adequate measure of the model's efficacy.

Practitioners and scholars can learn the accuracy, precision, recall, and overall efficacy of AD Detection and classification models by evaluating their efficacy using these standard metrics for assessment. The performance analysis report of the projected model is exposed in Table 2.

Table 2

Recital analysis of the proposed model

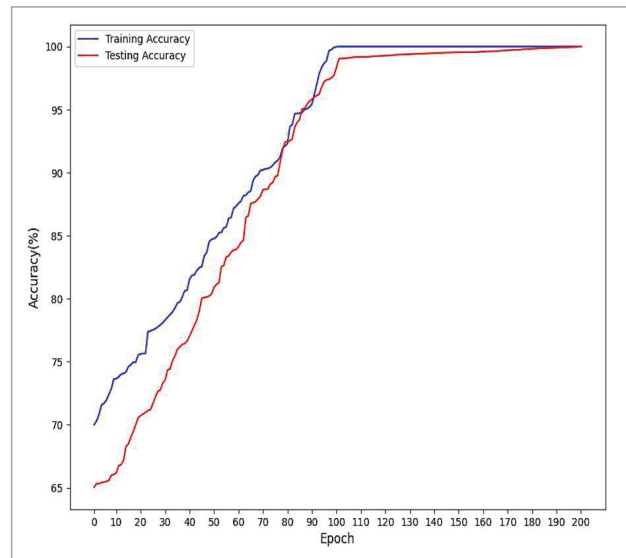
Class	Precision	Recall	F1-score
0	0.99	0.98	0.99
1	1.00	1.00	0.99
2	0.99	0.99	1.00
3	0.98	0.99	0.98
4	0.99	0.98	0.99
Accuracy	99.8		
Micro avg	0.99	0.99	0.99
Weighted avg	0.99	1.00	0.99

In Figure 5, the accuracy of the model for AD Detection is presented. The graph illustrates the training and testing accuracy achieved by the model during the training procedure. According to the graph, the model attained a training accuracy of 100%, indicating that it successfully predicted the correct class for all instances in the training dataset. This high training accuracy proposes that the model has effectively cultured the patterns and features present in the training data.

The testing accuracy, however, is shown to be 99.8%. Indicative of the algorithm's success in making accurate class predictions for instances in the testing dataset that it had not seen during training. Testing accuracy of 99.8% suggests that the model generaliz-

Figure 5

Accuracy of the DACN model for Alzheimer's Disease Detection



es well to unseen data and can effectively classify instances of Alzheimer's disease. The high training and testing accuracy indicate that the model has successfully learned the relevant patterns and features associated with Alzheimer's disease and can accurately classify new instances.

In Figure 6, the loss of the model during the training and testing phases is visualized. The training loss is represented as 0.02, indicating the average loss value

Figure 6

Loss of the DACN model for Alzheimer's Disease Detection

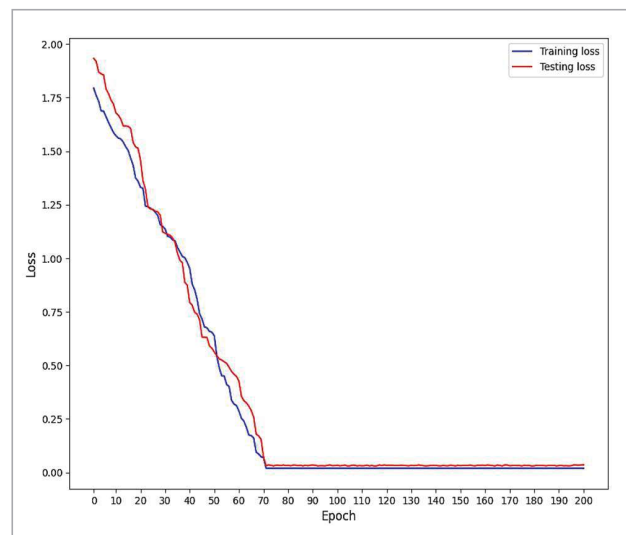
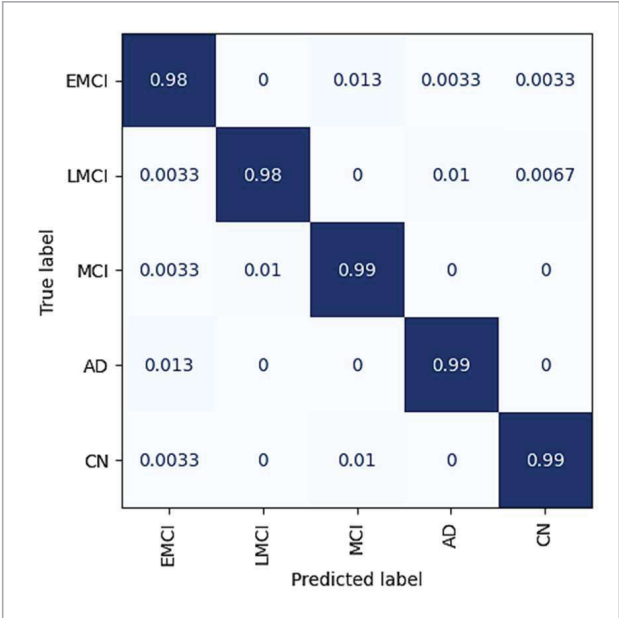


Figure 7
Confusion Matrix of the DACN Model for Alzheimer's Disease Detection



computed during the training process. On the other hand, the testing loss is shown as 0.03, meaning the average loss value is calculated during the testing or evaluation phase. The loss value indicates the model's performance level. It measures how far the model's forecasts deviate from the real ground-truth labels. The closer the model's forecasts are to the actual labels, the smaller the loss value. When the training loss is just 0.02, it is clear that the model is well-fit for the training data since it can reduce the error between anticipated and actual values. Similarly, a testing loss of 0.03 indicates that the model performs well on unobserved data during the testing phase, demonstrating its generalization capability.

Figure 7 presents a confusion matrix to evaluate the model's performance on different classes or categories, namely 'EMCI,' 'LMCI,' 'MCI,' 'AD,' and 'CN.' The confusion matrix is a graphical summary of how well the forecasts made by the model match the actual identifiers. The values in the confusion matrix are expressed as percentages and indicate the accuracy of the model's estimates for each class.

The model achieves an accuracy of 98% for predicting instances belonging to the 'EMCI' class. This means that out of all the cases that are true 'EMCI,' the model correctly classifies 98% of them, while 2% of 'EMCI'

instances are misclassified. The model achieves an accuracy of 98% for predicting instances belonging to the 'LMCI' class. This indicates that out of all the truly 'LMCI,' the model correctly classifies 98% of them, while 2% of 'LMCI' instances are misclassified. The model achieves an accuracy of 99% for predicting instances belonging to the 'MCI' class. This means that out of all the instances that are truly 'MCI,' the model correctly classifies 99% of them, while 1% of 'MCI' instances are misclassified.

The Area Under the ROC Curve (AUC) is a metric that enumerates the overall presentation of the model across all likely thresholds. AUC values range from 0 to 1, where 1 represents a flawless classifier. In our case, the classification model has exceptional performance with a ROC-AUC curve ranging from 0.99 to 1.00, as shown in Figure 8. This indicates that the model achieves near-perfect or perfect discrimination between the positive and negative classes, resulting in high predictive accuracy. AUC values in the range of 0.99 to 1.00 suggest that the model has excellent predictive power and can effectively differentiate between different classes.

Figure 8
The DACN model's ROC and Area Under the Curve for Classifying Alzheimer's

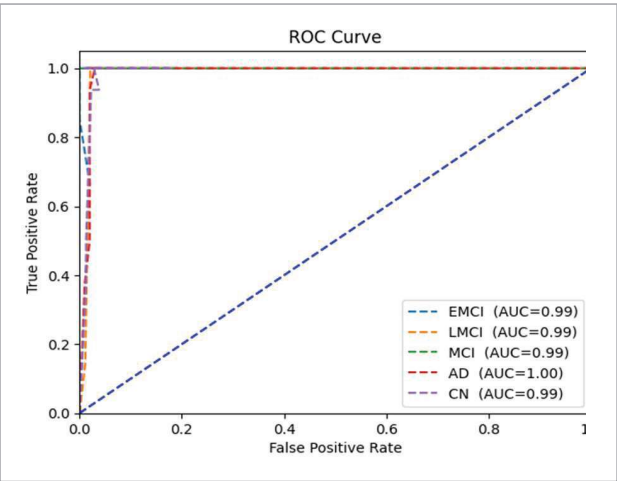


Table 3 summarizes the findings of an analysis of the suggested model and the baseline models used to analyze the same dataset. The table presents the performance metrics of different models, including CNN, LSTM, Bi-LSTM, CLSTM, ResNet50, and the proposed model. The metrics evaluated are accu-

Table 3

Performance comparison of the models on the dataset ADNI

Model	Accuracy	Precision	Recall	F1-score
CNN	95.6	0.95	0.94	0.95
LSTM	96.4	0.95	0.96	0.95
Bi-LSTM	94.8	0.95	0.94	0.95
CLSTM	96.9	0.97	0.96	0.97
ResNet50	97.5	0.97	0.96	0.96
Propose model	99.8	0.99	0.99	1.00

racy, precision, recall, and F1-score, which provide insights into the models' classification capabilities. The CNN model achieved an accuracy of 95.6% with precision, recall, and F1-score values of 0.95, 0.94, and 0.95, respectively. The LSTM model performed slightly better, with an accuracy of 96.4% and precision, recall, and F1-score values of 0.95, 0.96, and 0.95, respectively. The Bi-LSTM model achieved an accuracy of 94.8% with similar precision, recall, and F1-score values of 0.95, 0.94, and 0.95.

The CLSTM model showed improved performance, with an accuracy of 96.9% and precision, recall, and F1-score values of 0.97, 0.96, and 0.97. The ResNet50 model demonstrated even higher accuracy, reaching 97.5%, with precision, recall, and F1-score values of 0.97, 0.96, and 0.96. However, the proposed model outperformed all the baseline models, achieving an exceptional accuracy of 99.8%. The precision, recall and F1-score values were also remarkably high at 0.99, 0.99, and 1.00, respectively. This indicates that the proposed model excelled in accurately classifying instances of Alzheimer's

mer's disease, exhibiting superior performance compared to the baseline models. The results highlight the superiority of the proposed model in terms of accuracy and classification metrics. It demonstrates the model's ability to effectively identify Alzheimer's disease cases, outperforming other established models such as CNN, LSTM, Bi-LSTM, CLSTM, and ResNet50. These findings suggest that the proposed model holds promise as a highly accurate and reliable tool for AD detection on the given dataset.

Table 4 states various ablation studies in detail. The first model, without patching CNN segmentation on brain images, was done, and Dual Attention Aware Octave Convolution was performed for the final classification. In this model, image patching has not been done. CNN-based segmentation with Dual Attention Aware Octave Convolution has been done. The accuracy of the model is 97.5%, which is lower than the proposed model. Likewise, the second model, octave convolution and dual attention-based CNN, are processed without segmentation. Only images are trained and classified here using octave and double attention CNN. This model obtains 95% of accuracy. The third model is tested without octave convolution; in this model, we obtain an accuracy of 96.7%, which is lower than the first model. We tested dual attention CNN for training the images for the fourth model. In this model, initial neurons extract image features, and then, by further pooling, attention is used for classifying the image. Due to ineffective feature extraction, this model performs very low than other models. However, our proposal achieves better than all other models in the table. It is concluded that patching is the first essential component, followed by octave convolution, which extracts features on low and high

Table 4

Performance of Ablation models

Model	Accuracy	Precision	Recall	F1-score
CNN segmentation (No patching) + Dual Attention Aware Octave Convolution	97.5	96	96	97.4
Octave Convolution+dual attention CNN	97.8	97.3	97.6	97.2
PCNN+DACN	96.7	96.2	95.1	96
DACN	92.4	93.4	93.2	93.6
PCNN+OCTAVE+DACN (PROPOSED)	99.8	0.99	0.99	1.00

frequencies. Patching makes the images more evident by pointing out exact noises in image features. Octave convolution further improves image classification by efficiently capturing high-frequency and low-frequency information in an image. The removal of Octave convolution resulted in a noticeable decrease in the model's efficiency, highlighting its role in optimising computational resources. Conversely, the PCNN contributes to overall performance.

5. Conclusion and Future Work

This study concludes by presenting a deep learning-based method for automatically identifying AD using 3D brain MRI data. The study addresses the significant impact of brain illnesses, particularly AD, on fundamental human capabilities such as thought, speech, and movement. The proposed method, the dual

attention aware Octave convolution-based deep learning network (DACN), offers several key contributions. Firstly, it employs a PCNN to extract discriminative features from MRI patches while enhancing the detection of abnormally altered micro-structures in the brain. Secondly, an Octave convolution reduces spatial redundancy and improves the model's perception of the brain's structural details. Lastly, a dual attention-aware convolution classifier is employed to further analyze the resulting image representation. Experimental results using the publicly available ADNI dataset demonstrate the efficiency of the suggested model. The proposed method achieves an outstanding test accuracy of 99.87% for categorizing dementia phases, surpassing the recital of state-of-the-art models. This remarkable accuracy underscores the potential of the DACN model in accurately identifying Alzheimer's disease at an early stage. In future different datasets for AD can be implemented and tested for improving accuracy by cross verification.

References

1. Ahmed, S., Choi, K. Y., Lee, J. J., Kim, B. C., Kwon, G. R., Lee, K. H., Jung, H. Y. Ensembles of Patch-Based Classifiers for Diagnosing Alzheimer's Diseases. *IEEE Access*, 2019, 7, 73373-73383. <https://doi.org/10.1109/ACCESS.2019.2920011>
2. Balaji, P., Chaurasia, M. A., Bilfaqih, S. M., Muniasamy, A., Alsid, L. E. G. Hybridized Deep Learning Approach for Detecting Alzheimer's Disease. *Biomedicines*, 2023, 11(1), 149. <https://doi.org/10.3390/biomedicines11010149>
3. Ben Ahmed, O., Benois-Pineau, J., Allard, M., Ben Amar, C., Catheline, G. Alzheimer's Disease Neuroimaging Initiative. Classification of Alzheimer's Disease Subjects from MRI Using Hippocampal Visual Features. *Multimedia Tools and Applications*, 2015, 74, 1249-1266. <https://doi.org/10.1007/s11042-014-2123-y>
4. Braak, H., Braak, E. Frequency of Stages of Alzheimer-related Lesions in Different Age Categories. *Neurobiology of Aging*, 1997, 18(4), 351-357. [https://doi.org/10.1016/S0197-4580\(97\)00056-0](https://doi.org/10.1016/S0197-4580(97)00056-0)
5. Chen, Y., Fang, H., Xu, B., Yan, Z., Kalantidis, Y., Rohrbach, M., Yan, S., Feng, J. Drop an Octave: Reducing Spatial Redundancy in Convolutional Neural Networks with Octave Convolution. *arXiv 2019, arXiv:1904.05049*. <https://doi.org/10.1109/ICCV.2019.00353>
6. Dominy, S. S., Lynch, C., Ermini, F., Benedyk, M., Marczyk, A., Konradi, A., Nguyen, M., Haditsch, U., Raha, D., Griffin, C. Porphyromonas Gingivalis in Alzheimer's Disease Brains: Evidence for Disease Causation and Treatment with Small-Molecule Inhibitors. *Sci. Adv.* 2019, 5(1), eaau3333. <https://doi.org/10.1126/sciadv.aau3333>
7. El-Dahshan, E. S. A., Hosny, T., Salem, A. B. M. Hybrid Intelligent Techniques for MRI Brain Images Classification. *Digital Signal Processing*, 2010, 20(2), 433-441. <https://doi.org/10.1016/j.dsp.2009.07.002>
8. Fisher, D. W., Bennett, D. A., Dong, H. Sexual Dimorphism in Predisposition to Alzheimer's Disease. *Neurobiology of Aging*, 2018, 70, 308-324. <https://doi.org/10.1016/j.neurobiolaging.2018.04.004>
9. Förstl, H., Levy, R. On Certain Peculiar Diseases of Old Age. *History of Psychiatry*, 1991, 2, 71-101. <https://doi.org/10.1177/0957154X9100200505>
10. Gaugler, J., James, B., Johnson, T., Marin, A., Weuve, J. Alzheimer's Disease Facts and Figures. *Alzheimer's Dementia*, 2019, 15(3), 321-387. <https://doi.org/10.1016/j.jalz.2019.01.010>
11. Gray, K. R., Aljabar, P., Heckemann, R. A., Hammers, A. NeuroImage Random Forest-based Similarity Measures for Multi-Modal Classification of Alzheimer's Disease. *Neuroimage*, 2013, 65, 167-175. <https://doi.org/10.1016/j.neuroimage.2012.09.065>